AIMS Mathematics, 10(3): 6764–6787.
DOI:10.3934/math.2025310
Received: 17 January 2025
Revised: 14 March 2025
Accepted: 19 March 2025
Published: 26 March 2025

https://www.aimspress.com/journal/Math

Research article

A novel high-order symmetric and energy-preserving continuous-stage Runge-Kutta-Nyström Fourier pseudo-spectral scheme for solving the two-dimensional nonlinear wave equation

Dongjie Gao[1], Peiguo Zhang[1,*], Longqin Wang[2], Zhenlong Dai[3] and Yonglei Fang[4]

[1] School of Mathematics and Statistics, Heze University, Heze 274015, China

[2] School of Statistics and Data Science, Jiangsu normal University, Xuzhou 221116, China

[3] School of Information Engineering, Nanjing Xiaozhuang University, Nanjing 211171, China,

[4] School of Mathematics and Statistics, Zaozhuang University, Zaozhuang 277160, China

* **Correspondence:** Email: zhangpeiguo@163.com.

Abstract: The primary objective of this research is to develop a novel high-order symmetric and energy-preserving method for solving two-dimensional nonlinear wave equations. Initially, the nonlinear wave equation is reformulated as an abstract Hamiltonian ordinary differential equation (ODE) system with separable energy in an appropriate infinite-dimensional function space. Subsequently, an energy-preserving and symmetric continuous-stage Runge-Kutta-Nyström time-stepping scheme is derived. After approximating the spatial differential operator using the two-dimensional Fourier pseudo-spectral method, we derive an energy-preserving fully discrete scheme. A rigorous error analysis demonstrates that the proposed method can achieve at least fourth-order accuracy in time. Finally, numerical examples are provided to validate the accuracy, efficiency, and long-term energy conservation of the method.

Keywords: two dimensional nonlinear wave equations; energy-preserving method; symmetry; continuous-stage Runge-Kutta-Nyström method; Fourier pseudo-spectral method
Mathematics Subject Classification: 34C14, 65L06, 65L20, 65L70

1. Introduction

The nonlinear partial differential equations have significant roles in a variety of fields in engineering and science (see, e.g., [4, 39]), including quantum field theory, nonlinear optics, propagation of dislocations in crystals, nucleation, and solid state physics. In this paper, we consider the following

nonlinear wave equation in two dimensions:

$$\frac{\partial^2 u}{\partial t^2} - \kappa^2 \left(\frac{\partial^2 u}{\partial x^2} + \frac{\partial^2 u}{\partial y^2} \right) = f(u(x, y, t)), \quad (x, y) \in (0, L_1) \times (0, L_2), \quad t \in [t_0, T], \tag{1.1}$$

subject to the initial conditions

$$u(x, y, t_0) = \varphi_0(x, y), \quad \frac{\partial u}{\partial t}(x, y, t_0) = \varphi_1(x, y), \quad x \in [0, L_1] \times [0, L_2], \tag{1.2}$$

and the periodic boundary conditions

$$u(x, y, t) = u(x + L_1, y, t), \quad u(x, y, t) = u(x, y + L_2, t), \quad (x, y) \in \bar{\Omega}, \quad t \in [t_0, T], \tag{1.3}$$

where κ^2 is a dimensionless positive parameter, $\varphi_0(x, y)$ and $\varphi_1(x, y)$ are the given (L_1, L_2)- periodic functions, and L_1 and L_2 are the basic positive periods. In the literature, many works have been made to explore the analytical solution for the nonlinear wave equations (see, e.g., [1, 39]). However, it is difficult to obtain the general exact solutions for all the nonlinear wave equations. Therefore, the development of efficient and high-precision numerical methods for solving the two-dimensional nonlinear wave equations has became much more important. A great number of excellent numerical strategies have been proposed to study the nonlinear wave equations, including the finite difference methods (see, e.g., [12, 17, 18]), the finite element methods (see, e.g., [2, 3, 33]), the spectral methods [25], the domain decomposition methods [19], and the radial basis functions methods [11].

If the nonlinear function $f(u)$ is the negative derivative of a nonnegative function $F(u)$, i.e., $f(u) = -\frac{\mathrm{d}F(u)}{\mathrm{d}u}$, and the solution of (1.1) satisfies $(u, \frac{\partial u}{\partial t}) \in H^1(\Omega) \times L^2(\Omega)$, then the nonlinear wave Eqs (1.1)–(1.3) could conserve the energy

$$\begin{aligned} E(t) :=& \frac{1}{2} \int_\Omega \Big(u_t^2(x, y, t) + \kappa^2 \big| \nabla u(x, y, t) \big|^2 + 2F(u(x, y, t)) \Big) \mathrm{d}x\mathrm{d}y \\ \equiv& \frac{1}{2} \int_\Omega \Big(\varphi_1^2(x, y) + \kappa^2 \big| \nabla \varphi_0(x, y) \big|^2 + 2F(\varphi_0(x, y)) \Big) \mathrm{d}x\mathrm{d}y = E(t_0), \quad t \geq t_0. \end{aligned} \tag{1.4}$$

The energy conservation (1.4) is a significant property of the nonlinear wave equations, and plays prominent roles in investigating soliton theory. Under this case, the nonlinear wave equations like (1.1) are called nonlinear Hamiltonian wave equations. We know that the energy conservation along the exact flow is one most characteristic properties of the nonlinear Hamiltonian wave Eq (1.1). The energy-conserving numerical schemes usually yield correct physical phenomenons and numerical stability (see, e.g., [24, 29, 32]). Therefore, it will be meaningful to design suitable numerical schemes which could exactly preserve the discrete energy and symmetry of the nonlinear Hamiltonian wave Eq (1.1).

The development of energy-preserving numerical schemes for nonlinear Hamiltonian wave equations has garnered significant attention across various fields of mechanics. For example, Li et al. [21] proposed several finite difference schemes that preserve specific algebraic invariants of the nonlinear Klein-Gordon equations. Moreover, based on the concept of the discrete line integral method (see, e.g., [5, 6]), L. Brugnano et al. developed the energy-preserving Hamiltonian boundary value methods (HBVMs) to solve the nonlinear Hamiltonian PDEs (see, e.g., [7, 8]). The energy-preserving

average vector field (AVF) method was initially developed for solving Hamiltonian ordinary differential equations (ODEs). Recently, the AVF method, when combined with appropriate spatial semi-discretization techniques, has been utilized to numerically investigate nonlinear Hamiltonian wave equations, thereby attracting significant attention from researchers. For instance, AVF finite element methods have been introduced to solve one-dimensional Hamiltonian wave equations (see [10, 33]). In [31,32], combining the AVF method with the spatial fourth-order finite difference semidiscretisation, the authors developed energy-preserving methods for one- and two- dimensional Hamiltonian wave equations with Neumann boundary conditions. However, the previous schemes have only second-order accuracy in time. To enhance temporal accuracy, Hou et al. [17, 18] integrated the fourth-order AVF temporal integrator with spatial compact finite difference (CFD) discretization to construct and analyze high-order energy-preserving schemes for solving one- and two-dimensional nonlinear wave equations with variable coefficients. This represents a significant advancement in the field of energy-preserving methods for nonlinear Hamiltonian wave equations. Building on these contributions, we aim to develop and analyze a high-order energy-preserving and symmetric scheme for two-dimensional nonlinear Hamiltonian wave equations by combining the continuous-stage Runge-Kutta-Nyström time integrator with Fourier pseudo-spectral spatial discretization.

The rest of the paper is organized as follows: In Section 2, the two-dimensional nonlinear wave Eq (1.1) will first be reformulated as an abstract infinite-dimensional separable Hamiltonian ODE system in an appropriate function space. Then, the application of a continuous-stage Runge-Kutta-Nyström time integrator to the yielded ODE's system to derive the time-stepping scheme is presented. The energy preservation and symmetry of the proposed time-stepping scheme will be investigated. Furthermore, by approximating the spatial differential operator using the two-dimensional Fourier pseudo-spectral method, we derive a fully discrete scheme. A rigorous analysis of the energy conservation properties of this scheme is then conducted. The error analysis demonstrates that the proposed scheme achieves sixth-order accuracy in the relatively low regularity function space $C^2([t_0, T], \mathcal{B})$. Numerical experiments are presented in Section 4. Lastly, a concise conclusion is provided in Section 5.

2. Temporal semi-discretisation: energy-preserving and symmetric time-stepping scheme

In this section, we will first represent the two-dimensional nonlinear wave Eqs (1.1)–(1.3) as an abstract nonlinear ODE on an appropriate infinite-dimensional Hilbert space. Then, we will develop and analyze a novel energy-conserving time-stepping scheme for the abstract ODE.

2.1. Abstract Hamiltonian ODE's system

According to the analysis in references [30, 37], by defining the mapping

$$u(t) := [(x, y) \to u(x, y, t)],$$

we can express the nonlinear wave Eqs (1.1)–(1.3) as the following abstract ODE (e.g., [29, 30, 38]):

$$\begin{cases} u''(t) = -\mathcal{A}u(t) + f(u(t)) :\triangleq g(u(t)), & t \in [t_0, T], \\ u(t_0) = \varphi_0(x, y), \quad u'(t_0) = \varphi_1(x, y), & (x, y) \in \bar{\Omega}, \end{cases} \tag{2.1}$$

where $\mathcal{A}$ is the linear differential operator

$$\mathcal{A}u(t) = -\kappa^2 \Delta u(t), \quad \forall u(t) \in \mathcal{B},$$

and $\mathcal{B}$ is the infinite-dimensional Hilbert space

$$\mathcal{B} = \left\{ u \in H^2(\Omega) \ : \ u(x,y) = u(x+L_1,y), \ \ u(x,y) = u(x,y+L_2) \right\}. \tag{2.2}$$

For any $\phi(x,y), \psi(x,y) \in \mathcal{B}$, we introduce the inner product and the norms

$$(\phi(x,y), \psi(x,y)) = \int_\Omega \phi(x,y)\psi(x,y)\mathrm{d}x\mathrm{d}y, \quad \|\phi\| = \sqrt{(\phi(x,y), \phi(x,y))}, \quad |\phi|_1 = \sqrt{(-\Delta\phi(x,y), \phi(x,y))}.$$

Then, by taking the inner product of the abstract ODE's system (2.1) with $u'(t)$, we are able to find that system (2.1) can preserve the separable energy

$$\mathcal{H}[u(t), u'(t)] := \ \mathcal{H}_1[u'(t)] + \mathcal{H}_2[u(t)] \equiv \ \mathcal{H}_1[u'(t_0)] + \mathcal{H}_2[u(t_0)] = \mathcal{H}[u(t_0), u'(t_0)], \tag{2.3}$$

where the kinetic energy part $\mathcal{H}_1[u'(t)]$ and the potential energy part $\mathcal{H}_2[u(t)]$ are

$$\mathcal{H}_1[u'(t)] = \ \frac{1}{2}\left\|u'(t)\right\|^2 \quad \text{and} \quad \mathcal{H}_2[u'(t)] = \ \frac{\kappa^2}{2}\left|\nabla u(t)\right|_1^2 + \Big(F(u(t)), 1\Big), \tag{2.4}$$

respectively. Obviously, the energy $\mathcal{H}[u(t), u'(t)]$ of the abstract ODE (2.1) is the same as the energy $E(t)$ of the two-dimensional nonlinear wave Eqs (1.1)–(1.3). Moreover, the abstract ODE's system (2.1) is actually a Hamiltonian system

$$\frac{\mathrm{d}}{\mathrm{d}t}\begin{bmatrix} u(t) \\ v(t) \end{bmatrix} = \mathcal{S}\begin{bmatrix} \frac{\delta \mathcal{H}_2[u(t)]}{\delta u} \\ \frac{\delta \mathcal{H}_1[v(t)]}{\delta v} \end{bmatrix}, \tag{2.5}$$

where $v(t) = u'(t)$ and $\mathcal{S}$ is a skew-adjoint operator

$$\mathcal{S} = \begin{bmatrix} 0 & 1 \\ -1 & 0 \end{bmatrix}.$$

In light of the definition of the variational derivatives, we are able to check that

$$\frac{\delta \mathcal{H}_1[v(t)]}{\delta v} = v(t) \quad \text{and} \quad \frac{\delta \mathcal{H}_2[u(t)]}{\delta u} = \mathcal{A}u(t) - f(u(t)) = -g(u(t)). \tag{2.6}$$

The main purpose of this work is to design a suitable time-stepping scheme for the two-dimensional nonlinear wave Eqs (1.1)–(1.3), which could exactly preserve the separable energy $\mathcal{H}[u(t), u'(t)]$ or $E(t)$. To achieve this purpose, the temporal discretization strategy will be first considered for the abstract ODE (2.1) in the infinite-dimensional function space.

2.2. Formulation of the energy-preserving time-stepping scheme

For any positive integer N, we define the temporal mesh grid as

$$\Omega^N := \left\{ t_n \,\middle|\, t_n = t_0 + n\Delta t, \quad n = 0, 1, \ldots, N \right\} \tag{2.7}$$

with time step size $\Delta t = (T - t_0)/N$, and introduce the following approximations:

$$u^n \approx u(t_n), \qquad v^n \approx u'(t_n), \qquad U_\tau^n \approx u(t_n + \tau\Delta t), \quad \forall \tau \in [0, 1].$$

Then, applying the energy-preserving integrators, which are proposed for the second-order Hamiltonian ordinary differential systems (see [22, 26]), to the abstract ODEs (2.1), we can establish the time-stepping scheme for the two-dimensional nonlinear wave Eqs (1.1)–(1.3).

Definition 2.1. *For any one temporal single step t_n to t_{n+1}, a continuous-stage Runge-Kutta-Nyström (RKN) time-stepping scheme for the abstract ODE* (2.1) *is defined as*

$$\begin{cases} U_\tau^n = u^n + \tau\Delta t v^n + \Delta t^2 \displaystyle\int_0^1 P_{3,2}(\tau, \sigma) g(U_\sigma^n) \mathrm{d}\sigma, \\ u^{n+1} = u^n + \Delta t v^n + \Delta t^2 \displaystyle\int_0^1 (1 - \tau) g(U_\tau^n) \mathrm{d}\tau, \\ v^{n+1} = v^n + \Delta t \displaystyle\int_0^1 g(U_\tau^n) \mathrm{d}\tau, \end{cases} \tag{2.8}$$

where the weight function $P_{3,2}(\tau, \sigma)$ is a cubic binary polynomial of the form

$$P_{3,2}(\tau, \sigma) = \frac{\tau}{2}(1 - 6\sigma + 6\sigma^2 + 3\tau - 6\sigma^2\tau - 2\tau^2 + 4\sigma\tau^2), \qquad \forall (\tau, \sigma) \in [0, 1] \times [0, 1].$$

Remark 2.1. *In [22, 26], the authors introduced a framework for energy-preserving continuous-stage RKN methods for solving second-order Hamiltonian ODEs. Drawing upon the methodologies proposed in [22, 26], we develop a novel energy-preserving time-stepping scheme utilizing the weight function $P_{3,2}(\tau, \sigma)$, and extend this scheme to the two-dimensional nonlinear wave Eqs* (1.1)–(1.3). *Furthermore, it is important to emphasize that the selection of the weight function $P_{3,2}(\tau, \sigma)$ is not unique. Different choices of weight functions can result in numerical methods exhibiting varying accuracy.*

Now, we focus on verifying the energy conservation of the continuous-stage RKN time-stepping scheme defined in Definition 2.1 for the two-dimensional nonlinear wave Eqs (1.1)–(1.3).

Theorem 2.1. *The continuous-stage Runge-Kutta-Nyström time-stepping scheme* (2.8) *can exactly preserve the energy $\mathcal{H}[u(t), v(t)]$ of the two-dimensional nonlinear wave Eqs* (1.1)–(1.3) *or the infinite-dimensional abstract ODE's system* (2.1)*, that is,*

$$\mathcal{H}[u^{n+1}, v^{n+1}] \equiv \mathcal{H}[u^n, v^n], \qquad n = 0, 1, 2, \ldots, N - 1. \tag{2.9}$$

Proof. Noticing the form of the separable energy (2.3) and (2.4), we have

$$\mathcal{H}[u^{n+1}, v^{n+1}] = \mathcal{H}_1[v^{n+1}] + \mathcal{H}_2[u^{n+1}] = \frac{1}{2}(v^{n+1}, v^{n+1}) + \mathcal{H}_2[u^{n+1}]. \tag{2.10}$$

It follows from inserting the expression of v^{n+1} into (2.10) and after a careful calculation that

$$\begin{aligned}\mathcal{H}[u^{n+1}, v^{n+1}] &= \frac{1}{2}\Big(v^n + \Delta t \int_0^1 g(U_\tau^n)\mathrm{d}\tau, v^n + \Delta t \int_0^1 g(U_\tau^n)\mathrm{d}\tau\Big) + \mathcal{H}_2[u^{n+1}] \\ &= \mathcal{H}[u^n,v^n] + \Delta t\Big(v^n, \int_0^1 g(U_\tau^n)\mathrm{d}\tau\Big) + \frac{\Delta t^2}{2}\Big(\int_0^1 g(U_\tau^n)\mathrm{d}\tau, \int_0^1 g(U_\tau^n)\mathrm{d}\tau\Big) + \mathcal{H}_2[u^{n+1}] - \mathcal{H}_2[u^n].\end{aligned} \tag{2.11}$$

Moreover, it is evident that

$$\mathcal{H}_2[u^{n+1}] - \mathcal{H}_2[u^n] = \int_0^1 \mathrm{d}\mathcal{H}_2[U_\tau^n] = \int_0^1 \Big(\frac{\delta \mathcal{H}_2[U_\tau^n]}{\delta u}, \frac{\mathrm{d}U_\tau^n}{\mathrm{d}\tau}\Big)\mathrm{d}\tau = -\int_0^1 \Big(g(U_\tau^n), \frac{\mathrm{d}U_\tau^n}{\mathrm{d}\tau}\Big)\mathrm{d}\tau. \tag{2.12}$$

Substituting the expressions of U_τ^n into (2.12) leads to

$$\begin{aligned}\mathcal{H}_2[u^{n+1}] - \mathcal{H}_2[u^n] &= -\int_0^1 \Big(g(U_\tau^n), \Delta t v^n + \Delta t^2 \int_0^1 \frac{\partial P_{3,2}(\tau,\sigma)}{\partial \tau} g(U_\sigma^n)\mathrm{d}\sigma\Big)\mathrm{d}\tau \\ &= -\Delta t\Big(v^n, \int_0^1 g(U_\tau^n)\mathrm{d}\tau\Big) - \Delta t^2 \int_0^1 \Big(g(U_\tau^n), \int_0^1 \frac{\partial P_{3,2}(\tau,\sigma)}{\partial \tau} g(U_\sigma^n)\mathrm{d}\sigma\Big)\mathrm{d}\tau.\end{aligned} \tag{2.13}$$

Noticing the form of the weight function $P_{3,2}(\tau,\sigma)$, we have

$$\frac{\partial P_{3,2}(\tau,\sigma)}{\partial \tau} = \frac{1}{2} - 3\sigma + 3\tau + 3\sigma^2 - 3\tau^2 - 6\sigma^2\tau + 6\sigma\tau^2, \qquad \forall (\tau,\sigma) \in [0,1]\times[0,1].$$

Therefore, Eq (2.13) can be simplified as

$$\mathcal{H}_2[u^{n+1}] - \mathcal{H}_2[u^n] = -\Delta t\Big(v^n, \int_0^1 g(U_\tau^n)\mathrm{d}\tau\Big) - \frac{\Delta t^2}{2}\Big(\int_0^1 g(U_\tau^n)\mathrm{d}\tau, \int_0^1 g(U_\sigma^n)\mathrm{d}\sigma\Big). \tag{2.14}$$

Comparing (2.11) with (2.14), we obtain

$$\mathcal{H}[u^{n+1}, u'^{n+1}] \equiv \mathcal{H}[u^n, u'^n], \qquad n = 0, 1, 2, \ldots, N-1.$$

The conclusion of the theorem is confirmed. □

The symmetric time integration method usually exhibits superior long time computational behavior along the numerical flows (see Chapter V in [16]). We know that the two-dimensional nonlinear wave Eqs (1.1)–(1.3) are temporal reversible (see, e.g., [24, 28, 29]). Therefore, it will be significant to investigate the symmetry of the energy-preserving continuous stage RKN time-stepping scheme.

Theorem 2.2. *The energy-preserving continuous-stage Runge-Kutta-Nyström time-stepping scheme* (2.1) *for solving the two-dimensional nonlinear wave Eqs* (1.1)–(1.3) *is temporal reversible.*

Proof. According to the concept of the time reversible integration method (see Chapter V in [16]), and applying the following transformations

$$\Delta t \leftrightarrow -\Delta t, \qquad u^{n+1} \leftrightarrow u^n, \qquad v^{n+1} \leftrightarrow v^n, \qquad \tau = 1 - \tau$$

to the time-stepping scheme (2.1), we obtain the adjoint scheme

$$\begin{cases} U^n_{1-\tau} = u^{n+1} - (1-\tau)\Delta t v^{n+1} + \Delta t^2 \int_0^1 P_{3,2}(1-\tau,\sigma) g(U^n_\sigma) \mathrm{d}\sigma, \\ u^n = u^{n+1} - \Delta t v^{n+1} + \Delta t^2 \int_0^1 \sigma g(U^n_\sigma) \mathrm{d}\sigma, \\ v^n = v^{n+1} - \Delta t \int_0^1 g(U^n_\sigma) \mathrm{d}\sigma. \end{cases} \tag{2.15}$$

After a careful calculation, the last two equations of the adjoint scheme (2.15) can be rewritten as

$$\begin{cases} u^{n+1} = u^n + \Delta t v^n + \Delta t^2 \int_0^1 \sigma g(U^n_\sigma) \mathrm{d}\sigma, \\ v^{n+1} = v^n + \Delta t \int_0^1 g(U^n_\sigma) \mathrm{d}\sigma. \end{cases} \tag{2.16}$$

Inserting Eq (2.16) into the first equation of (2.15), we obtain

$$U^n_{1-\tau} = u^n + \tau \Delta t v^n + \Delta t^2 \int_0^1 (\sigma - (1-\tau) + P_{3,2}(1-\tau,\sigma)) g(U^n_\sigma) \mathrm{d}\sigma. \tag{2.17}$$

The integral transformation $\tau = 1 - \xi$ yields that

$$1 - \xi - (1-\tau) + P_{3,2}(1-\tau, 1-\xi) = P_{3,2}(\tau,\xi). \tag{2.18}$$

Therefore, we see that the adjoint scheme (2.15) is the same as scheme (2.8). That means the energy-preserving continuous stage RKN time-stepping scheme is symmetric or temporal reversible. □

Utilizing the variation-of-constants formula on the infinite-dimensional abstract ODE system (2.1), the exact solution of the abstract system (2.1) can be expressed as

$$u(t_n + \tau\Delta t) = u(t_n) + \tau \Delta t v(t_n) + \Delta t^2 \int_0^\tau (\tau - \sigma) g(u(t_n + \sigma \Delta t)) \mathrm{d}\sigma, \quad \forall \tau \in [0,1]. \tag{2.19}$$

Furthermore, it is easy to obtain from Eq (2.19) that

$$\begin{cases} u(t_{n+1}) = u(t_n) + \Delta t v(t_n) + \Delta t^2 \int_0^1 (1-\tau) g(u(t_n + \tau\Delta t)) \mathrm{d}\tau, \\ v(t_{n+1}) = v(t_n) + \Delta t \int_0^1 g(u(t_n + \tau\Delta t)) \mathrm{d}\tau. \end{cases} \tag{2.20}$$

Inserting the exact solution $u(t)$ of the infinite-dimensional abstract ODE system (2.1) into the time-stepping scheme (2.8), we have

$$\begin{cases} u(t_n + \tau\Delta t) = u(t_n) + \tau \Delta t v(t_n) + \Delta t^2 \int_0^1 P_{3,2}(\tau,\sigma) g(u(t_n + \sigma\Delta t)) \mathrm{d}\sigma + R^n(\tau), \\ u(t_{n+1}) = u(t_n) + \Delta t v(t_n) + \Delta t^2 \int_0^1 (1-\tau) g(u(t_n + \tau\Delta t)) \mathrm{d}\tau, \\ v(t_{n+1}) = v(t_n) + \Delta t \int_0^1 g(u(t_n + \tau\Delta t)) \mathrm{d}\tau, \end{cases} \tag{2.21}$$

where the residual $R^n(\tau)$ is a function of $\tau \in [0,1]$. Applying the Taylor expansion with integral remainder

$$u(t_n + \sigma\Delta t) = u(t_n) + \sigma\Delta t v(t_n) + \Delta t^2 \int_0^\sigma (\sigma - z)u''(t_n + z\Delta t)\mathrm{d}z \tag{2.22}$$

to the nonlinear integrands appearing in (2.19) and the first equation of (2.21) results in

$$u(t_n+\tau\Delta t) = u(t_n)+\tau\Delta t v(t_n)+\Delta t^2 \int_0^\tau (\tau-\sigma)g\Big(u(t_n)+\sigma\Delta t v(t_n)+\Delta t^2 \int_0^\sigma (\sigma-z)u''(t_n+z\Delta t)\mathrm{d}z\Big)\mathrm{d}\sigma, \tag{2.23}$$

and

$$u(t_n+\tau\Delta t) = u(t_n)+\tau\Delta t v(t_n)+\Delta t^2\int_0^1 P_{3,2}(\tau,\sigma)g\Big(u(t_n)+\sigma\Delta t v(t_n)+\Delta t^2\int_0^\sigma (\sigma-z)u''(t_n+z\Delta t)\mathrm{d}z\Big)\mathrm{d}\sigma+R^n(\tau). \tag{2.24}$$

Comparing the formulae (2.23) with (2.24), and noticing $g(u) = -\mathcal{A}u + f(u)$, we can approximate the local residuals $R^n(\tau)$, $0 \le \tau \le 1$, in the following theorem.

Theorem 2.3. *Suppose that the exact solution u of the abstract ODE's system* (2.1) *satisfies $u \in C^2([t_0, T], \mathcal{B})$ and the nonlinear function $f' \in L^\infty([t_0, T], \mathcal{B})$. Then, the remainder $R^n(\tau)$ satisfies the estimations*

$$\|R^n(\tau)\| \le C\Delta t^4, \qquad 0 \le \tau \le 1, \tag{2.25}$$

where C is a constant and independent of Δt.

Proof. Subtracting (2.24) from (2.23) and noticing $g(u) = -\mathcal{A}u + f(u)$, we obtain

$$R^n(\tau) = \Theta_1^n(\tau) + \Theta_2^n(\tau), \tag{2.26}$$

where

$$\begin{aligned}\Theta_1^n(\tau) = & -\Delta t^2 \int_0^\tau (\tau - \sigma)\mathcal{A}\Big(u(t_n) + \sigma\Delta t v(t_n) + \Delta t^2 \int_0^\sigma (\sigma - z)u''(t_n + z\Delta t)\mathrm{d}z\Big)\mathrm{d}\sigma \\ & + \Delta t^2 \int_0^1 P_{3,2}(\tau,\sigma)\mathcal{A}\Big(u(t_n) + \sigma\Delta t v(t_n) + \Delta t^2 \int_0^\sigma (\sigma - z)u''(t_n + z\Delta t)\mathrm{d}z\Big)\mathrm{d}\sigma,\end{aligned} \tag{2.27}$$

and

$$\begin{aligned}\Theta_2^n(\tau) = & \Delta t^2 \int_0^\tau (\tau - \sigma)f\Big(u(t_n) + \sigma\Delta t v(t_n) + \Delta t^2 \int_0^\sigma (\sigma - z)u''(t_n + z\Delta t)\mathrm{d}z\Big)\mathrm{d}\sigma \\ & - \Delta t^2 \int_0^1 P_{3,2}(\tau,\sigma)f\Big(u(t_n) + \sigma\Delta t v(t_n) + \Delta t^2 \int_0^\sigma (\sigma - z)u''(t_n + z\Delta t)\mathrm{d}z\Big)\mathrm{d}\sigma.\end{aligned} \tag{2.28}$$

It follows from the definition of the bilinear polynomial weight function $P_{3,2}(\tau,\sigma)$ that

$$\int_0^\tau (\tau - \sigma)\mathrm{d}\sigma = \int_0^1 P_{3,2}(\tau,\sigma)\mathrm{d}\sigma = \frac{\tau^2}{2} \quad \text{and} \quad \int_0^\tau \sigma(\tau - \sigma)\mathrm{d}\sigma = \int_0^1 \sigma P_{3,2}(\tau,\sigma)\mathrm{d}\sigma = \frac{\tau^3}{6}. \tag{2.29}$$

Therefore, it is easy to check that

$$\Theta_1^n(\tau) = -\Delta t^4\int_0^\tau\int_0^\sigma (\tau-\sigma)(\sigma-z)\mathcal{A}u''(t_n+z\Delta t)\mathrm{d}z\mathrm{d}\sigma+\Delta t^4\int_0^1\int_0^\sigma P_{3,2}(\tau,\sigma)(\sigma-z)\mathcal{A}u''(t_n+z\Delta t)\mathrm{d}z\mathrm{d}\sigma. \tag{2.30}$$

Utilizing the Taylor expansion of $f(\cdot)$, i.e.,

$$f\Big(u(t_n)+\sigma\Delta t v(t_n)+\Delta t^2\int_0^\sigma(\sigma-z)u''(t_n+z\Delta t)\mathrm{d}z\Big)=f(u(t_n))+f'(u(t_n))\Big(\sigma\Delta t v(t_n)+\Delta t^2\int_0^\sigma(\sigma-z)u''(t_n+z\Delta t)\mathrm{d}z\Big)+\cdots$$

in (2.28) and recalling Eq (2.29), we have

$$\begin{aligned}\Theta_2^n(\tau) = {} & \Delta t^4 f'(u(t_n))\int_0^\tau\int_0^\sigma(\tau-\sigma)(\sigma-z)u''(t_n+z\Delta t)\mathrm{d}z\mathrm{d}\sigma \\ & -\Delta t^4 f'(u(t_n))\int_0^1\int_0^\sigma P_{3,2}(\tau,\sigma)(\sigma-z)u''(t_n+z\Delta t)\mathrm{d}z\mathrm{d}\sigma+O(\Delta t^5).\end{aligned} \tag{2.31}$$

Inserting the results (2.30) and (2.31) into (2.26), and taking the L^2 norms on both sides of (2.29), it is easy to verify the estimated result of the theorem.

□

3. Structure-preserving fully discrete scheme

In this section, by combing the Fourier pseudo-spectral spatial approximation with the continuous-stage RKN time-stepping scheme (2.8), we will construct the energy-preserving fully discrete scheme for the two-dimensional nonlinear wave Eqs (1.1) and (1.2).

Choose M_1 and M_2 to be any even integers, and define $\Delta x := \frac{L_1}{M_1}$ and $\Delta y := \frac{L_2}{M_2}$ as the spatial steps. Then, the temporal-spatial grid points are denoted as $\Omega_M^N = \Omega_M \times \Omega^N$, where the temporal grid Ω^N is given by (2.7), and the spatial grid Ω_M is defined as

$$\Omega_M := \Big\{(x_j,x_k)\ \Big|\ x_j = j\Delta x,\ j=0,1,\ldots,M_1-1,\ \ y_k = k\Delta y,\ k=0,1,\ldots,M_2-1\Big\}. \tag{3.1}$$

The grid function space $\mathbb{V}_M$ defined on Ω_M is given by

$$\mathbb{V}_M = \Big\{u\ \Big|\ u=(u_{j,k})\ \text{ with }\ u_{j,k}=u(x_j,y_k),\ \ (x_j,y_k)\in\Omega_M\Big\}.$$

For any $u=(u_{j,k})\in\mathbb{V}_M$, we can reformulate it as the vector form

$$\mathbf{u} = (u_{0,0},\cdots,u_{M_1-1,0},u_{0,1},\cdots,u_{M_1-1,1},\cdots,u_{0,M_2-1},\cdots,u_{M_1-1,M_2-1})^\top.$$

Therefore, the vector space of the grid functions $\mathcal{V}_M$, which is identical to $\mathbb{V}_M$, can be presented as

$$\mathcal{V}_M = \Big\{\mathbf{u}\ \Big|\ \mathbf{u} = (u_{0,0},\cdots,u_{M_1-1,0},u_{0,1},\cdots,u_{M_1-1,1},\cdots,u_{0,M_2-1},\cdots,u_{M_1-1,M_2-1})^\top\ \text{ with }\ u=(u_{j,k})\in\mathbb{V}_M\Big\}.$$

In addition, the corresponding discrete inner product and norm are defined as

$$\langle\mathbf{u},\mathbf{v}\rangle = \Delta x\Delta y\sum_{j=0}^{M_1-1}\sum_{k=0}^{M_2-1}u_{j,k}^n v_{j,k}^n,\qquad \|\mathbf{u}\| = \sqrt{\langle\mathbf{u},\mathbf{u}\rangle},\qquad \forall\mathbf{u},\mathbf{v}\in\mathcal{V}_M.$$

3.1. Spatial semi-discretisation: Fourier pseudo-spectral method

Define the interpolation space as

$$\mathcal{S}_M^p := \text{span}\Big\{g_j(x)g_k(y),\ \ 0 \le j \le M_1 - 1,\ 0 \le k \le M_2 - 1\Big\},$$

where $g_j(x)$ and $g_k(y)$ are trigonometric polynomials

$$g_j(x) = \frac{1}{M_1}\sum_{k_1=-M_1/2}^{M_1/2}\frac{1}{c_{k_1}}e^{\mathbf{i}k_1\mu_1(x-x_j)}, \qquad g_k(y) = \frac{1}{M_2}\sum_{k_2=-M_2/2}^{M_2/2}\frac{1}{c_{k_2}}e^{\mathbf{i}k_2\mu_2(y-y_k)}$$

with $\mu_1 = \frac{2\pi}{L_1}$, $\mu_2 = \frac{2\pi}{L_2}$, and

$$c_{k_1} = \begin{cases}1, & |k_1| < M_1/2,\\ 2, & |k_1| = M_1/2,\end{cases} \qquad c_{k_2} = \begin{cases}1, & |k_2| < M_2/2,\\ 2, & |k_2| = M_2/2.\end{cases}$$

Therefore, for any periodic function $u(x, y) \in L_p^2(\Omega)$, the interpolation operator $I_M : L_p^2(\Omega) \to \mathcal{S}_M^p$ is

$$I_M u(x,y) = \sum_{j=0}^{M_1-1}\sum_{k=0}^{M_2-1} u(x_j, y_k)g_j(x)g_k(x) = \sum_{k_1=-M_1/2}^{M_1/2}\sum_{k_2=-M_2/2}^{M_2/2}\tilde{u}_{k_1,k_2}e^{\mathbf{i}k_1\mu_1 x}e^{\mathbf{i}k_2\mu_2 y}, \tag{3.2}$$

where the Fourier coefficients $\tilde{u}_{k_1,k_2}$ are

$$\tilde{u}_{k_1,k_2} = \frac{1}{M_1 c_{k_1}}\frac{1}{M_2 c_{k_2}}\sum_{l=0}^{M_1-1}\sum_{k=0}^{M_2-1} u(x_l, y_k)e^{-\mathbf{i}k_1\mu_1 x_l}e^{-\mathbf{i}k_2\mu_2 y_k}. \tag{3.3}$$

Moreover, it is simple to check that

$$\tilde{u}_{-M_1/2,\cdot} = \tilde{u}_{M_1/2,\cdot} \qquad \text{and} \qquad \tilde{u}_{\cdot,-M_2/2} = \tilde{u}_{\cdot,M_2/2}.$$

It follows from applying the differential operator $\mathcal{A}$ to the interpolation $I_M u(x, y)$ that

$$\begin{aligned}\mathcal{A}I_M u(x,y)\big|_{x=x_i,y=y_j} &= \sum_{k_1=-M_1/2}^{M_1/2}\sum_{k_2=-M_2/2}^{M_2/2}\kappa^2[(\mu_1 k_1)^2 + (\mu_2 k_2)^2]\tilde{u}_{k_1,k_2}e^{\mathbf{i}k_1\mu_1 x_i}e^{\mathbf{i}k_2\mu_2 y_j}\\ &= \sum_{k_2=-M_1/2}^{M_1/2}\left(\sum_{k_1=-M_2/2}^{M_2/2}\kappa^2(\mu_1 k_1)^2\tilde{u}_{k_1,k_2}e^{\mathbf{i}k_1\mu_1 x_i}\right)e^{\mathbf{i}k_2\mu_2 y_j}\\ &\quad + \sum_{k_1=-M_2/2}^{M_2/2}\left(\sum_{k_2=-M_1/2}^{M_1/2}\kappa^2(\mu_2 k_2)^2\tilde{u}_{k_1,k_2}e^{\mathbf{i}k_2\mu_2 y_j}\right)e^{\mathbf{i}k_1\mu_1 x_i}\\ &= \Big((I_{M_2}\otimes D_2^x + D_2^y\otimes I_{M_1})\mathbf{u}\Big)_{i,j},\end{aligned} \tag{3.4}$$

where $I_{M_i}, i = 1, 2$ are the unity matrices, and $D_2^x = F_{M_1}^H\Lambda_1 F_{M_1}$ and $D_2^y = F_{M_2}^H\Lambda_2 F_{M_2}$ are the spectral differential matrices. Here, we should point out that F_M is the discrete Fourier transform matrix with

elements $(F_M)_{j,k} = \frac{1}{\sqrt{M}} e^{\frac{-2\pi \mathrm{i}(j)(k)}{M}}$, $j,k = 0,1,\ldots,M-1$, F_M^H is the conjugate transformation matrix of F_M, and Λ_1, Λ_2 are the frequency matrices with entries

$$\begin{aligned} \Lambda_1 &= \mathrm{diag}(\lambda_{D_2^x,0}, \lambda_{D_2^x,1}, \ldots, \lambda_{D_2^x,M_1-1}), \quad \lambda_{D_2^x,j} = \begin{cases} \kappa^2(\mu_1 j)^2, & 0 \le j \le M_1/2, \\ \kappa^2(\mu_1(j-M_1))^2, & M_1/2 < j \le M_1 - 1, \end{cases} \\ \Lambda_2 &= \mathrm{diag}(\lambda_{D_2^y,0}, \lambda_{D_2^y,1}, \ldots, \lambda_{D_2^y,M_2-1}), \quad \lambda_{D_2^y,j} = \begin{cases} \kappa^2(\mu_2 j)^2, & 0 \le j \le M_2/2, \\ \kappa^2(\mu_2(j-M_2))^2, & M_2/2 < j \le M_2 - 1. \end{cases} \end{aligned} \tag{3.5}$$

Thus, the spectral differential matrix A for approximating the 2D differential operator $\mathcal{A}$ can be expressed as (see, e.g., [13, 14, 40])

$$\begin{aligned} A\mathbf{u} =& (I_{M_2} \otimes D_2^x + D_2^y \otimes I_{M_1})\mathbf{u} \\ =& (F_{M_2}^H I_{M_2} F_{M_2} \otimes F_{M_1}^H \Lambda_1 F_{M_1} + F_{M_2}^H \Lambda_2 F_{M_2} \otimes F_{M_1}^H I_{M_1} F_{M_1})\mathbf{u} \\ =& \Big((F_{M_2} \otimes F_{M_1})^H (I_{M_2} \otimes \Lambda_1)(F_{M_2} \otimes F_{M_1}) + (F_{M_2} \otimes F_{M_1})^H (\Lambda_2 \otimes I_{M_1})(F_{M_2} \otimes F_{M_1})\Big)\mathbf{u} \\ =& \Big((F_{M_2} \otimes F_{M_1})^H (I_{M_2} \otimes \Lambda_1 + \Lambda_2 \otimes I_{M_1})(F_{M_2} \otimes F_{M_1})\Big)\mathbf{u}. \end{aligned} \tag{3.6}$$

Actually, the spectral differential matrix A is a symmetric and semi-positive matrix, and $A\mathbf{u}$ can be fast computed by the two-dimensional FFT function ifft2($\Lambda .*$ fft2($\mathbf{u}$)) built in MATLAB.

Using the spectral differential matrix A to approximate the differential operator $\mathcal{A}$, the two-dimensional nonlinear wave Eqs (1.1) and (1.2) or the abstract ODE system (2.1) can be converted into the semi-discrete system

$$\begin{cases} \mathbf{u}''(t) = g(\mathbf{u}(t)), & t \in [t_0, T], \\ \mathbf{u}(t_0) = \varphi_0, \quad \mathbf{u}'(t_0) = \varphi_1, \end{cases} \tag{3.7}$$

where $\mathbf{u}(t) \in \mathcal{V}_M$ and $g(\mathbf{u}(t)) = -A\mathbf{u}(t) + f(\mathbf{u}(t))$ with

$$f(\mathbf{u}(t)) = \Big(f(u_{0,0}(t)), \cdots, f(u_{M_1-1,0}(t)), f(u_{0,1}(t)), \cdots, f(u_{M_1-1,1}(t)), \cdots, f(u_{0,M_2-1}(t)), \cdots, f(u_{M_1-1,M_2-1}(t))\Big)^\top.$$

Taking the discrete inner product on both sides of the semi-discrete system (3.7) with $\mathbf{u}'(t)$, we have

$$\Big\langle \mathbf{u}''(t), \mathbf{u}'(t) \Big\rangle + \Big\langle A\mathbf{u}(t), \mathbf{u}'(t) \Big\rangle - \Big\langle f(\mathbf{u}(t)), \mathbf{u}'(t) \Big\rangle = 0,$$

which means

$$\frac{\mathrm{d}}{\mathrm{d}t}\left(\frac{1}{2}\Big\langle \mathbf{u}'(t), \mathbf{u}'(t) \Big\rangle + \frac{1}{2}\Big\langle A\mathbf{u}(t), \mathbf{u}(t) \Big\rangle + \Big\langle F(\mathbf{u}(t)), 1 \Big\rangle\right) = 0.$$

Therefore, we can conclude that the semi-discrete system (3.7) is energy-conserving.

Theorem 3.1. *Suppose that $\mathbf{u}(t) \in \mathcal{V}_M$ is the solution of the semi-discrete system* (3.7)*. Then, the semi-discrete system* (3.7) *can conserve the discrete energy*

$$H[\mathbf{u}(t), \mathbf{u}'(t)] := H_1[\mathbf{u}'(t)] + H_2[\mathbf{u}(t)], \tag{3.8}$$

where the discrete kinetic energy $H_1[\mathbf{u}'(t)]$ and discrete potential energy $H_2[\mathbf{u}(t)]$ are given by

$$H_1[\mathbf{u}'(t)] = \frac{1}{2}\Big\langle \mathbf{u}'(t), \mathbf{u}'(t) \Big\rangle \qquad \textit{and} \qquad H_2[\mathbf{u}(t)] = \frac{1}{2}\Big\langle A\mathbf{u}(t), \mathbf{u}(t) \Big\rangle + \Big\langle F(\mathbf{u}(t)), 1 \Big\rangle. \tag{3.9}$$

Proof. The proof process is straightforward along the above analysis. Therefore, we omit the details. □

Remark 3.1. *Actually, the energies* (3.8) *and* (3.9) *the discrete versions of the energies* (2.3) *and* (2.4) *of the the two-dimensional nonlinear wave Eqs* (1.1) *and* (1.2) *or the abstract system* (2.1)*. Therefore, we will explore the fully discrete scheme which can exactly preserve the discrete energies* (3.8) *and* (3.9) *in this work.*

3.2. Energy-preserving fully discrete scheme

The main strategy of the construction of the energy-preserving fully discrete scheme is to approximate the differential operator $\mathcal{A}$ in the continuous-stage RKN time-stepping scheme (2.8) by the spectral differential matrix A. Therefore, the following theorem will show that the fully discrete scheme could preserve the discrete energy (3.8) and (3.9) exactly.

Theorem 3.2. *By following the continuous stage RKN Fourier pseudo-spectral scheme*

$$\begin{cases} \mathbf{U}_\tau^n = \mathbf{u}^n + \tau\Delta t\mathbf{v}^n + \Delta t^2 \int_0^1 P_{3,2}(\tau,\sigma) g(\mathbf{U}_\sigma^n)\mathrm{d}\sigma, \\ \mathbf{u}^{n+1} = \mathbf{u}^n + \Delta t\mathbf{v}^n + \Delta t^2 \int_0^1 (1-\tau) g(\mathbf{U}_\tau^n)\mathrm{d}\tau, \\ \mathbf{v}^{n+1} = \mathbf{v}^n + \Delta t \int_0^1 g(\mathbf{U}_\tau^n)\mathrm{d}\tau, \end{cases} \tag{3.10}$$

with $g(u) = -Au + f(u)$ and Δt the time step size, the discrete energies (3.8) *and* (3.9) *are conserved, i.e.,*

$$H[\mathbf{u}^{n+1}, \mathbf{v}^{n+1}] = H[\mathbf{u}^n, \mathbf{v}^n]. \tag{3.11}$$

Proof. We calculate the separable energy

$$H[\mathbf{u}^{n+1}, \mathbf{v}^{n+1}] = H_1[\mathbf{v}^{n+1}] + H_2[\mathbf{u}^{n+1}]. \tag{3.12}$$

Inserting $\mathbf{v}^{n+1}$ into $H_1[\mathbf{v}^{n+1}]$ and keeping that A is a symmetric matrix in mind gives

$$\begin{aligned} H_1[\mathbf{v}^{n+1}] =& \frac{1}{2}\Big\langle \mathbf{v}^{n+1}, \mathbf{v}^{n+1}\Big\rangle = \frac{1}{2}\Big\langle \mathbf{v}^n + \Delta t\int_0^1 g(\mathbf{U}_\tau^n)\mathrm{d}\tau, \mathbf{v}^n + \Delta t\int_0^1 g(\mathbf{U}_\tau^n)\mathrm{d}\tau\Big\rangle \\ =& \frac{1}{2}\Big\langle \mathbf{v}^n, \mathbf{v}^n\Big\rangle + \Delta t\Big\langle \mathbf{v}^n, \int_0^1 g(\mathbf{U}_\tau^n)\mathrm{d}\tau\Big\rangle + \frac{\Delta t^2}{2}\Big\langle \int_0^1 g(\mathbf{U}_\tau^n)\mathrm{d}\tau, \int_0^1 g(\mathbf{U}_\tau^n)\mathrm{d}\tau\Big\rangle \\ =& H_1[\mathbf{v}^n] + \Delta t\Big\langle \mathbf{v}^n, \int_0^1 g(\mathbf{U}_\tau^n)\mathrm{d}\tau\Big\rangle + \frac{\Delta t^2}{2}\Big\langle \int_0^1 g(\mathbf{U}_\tau^n)\mathrm{d}\tau, \int_0^1 g(\mathbf{U}_\tau^n)\mathrm{d}\tau\Big\rangle. \end{aligned} \tag{3.13}$$

On the other hand, we have

$$\begin{aligned} H_2[\mathbf{u}^{n+1}] - H_2[\mathbf{u}^n] =& \int_0^1 \mathrm{d}H_2[\mathbf{U}_\tau^n] = -\int_0^1 \Big\langle g(\mathbf{U}_\tau^n), \frac{\mathrm{d}\mathbf{U}_\tau^n}{\mathrm{d}\tau}\Big\rangle\mathrm{d}\tau \\ =& -\int_0^1 \Big\langle g(\mathbf{U}_\tau^n), \Delta t\mathbf{v}^n + \Delta t^2\int_0^1 \frac{\partial P_{3,2}(\tau,\sigma)}{\partial\tau} g(\mathbf{U}_\sigma^n)\mathrm{d}\sigma\Big\rangle\mathrm{d}\tau. \end{aligned} \tag{3.14}$$

It follows from inserting

$$\frac{\partial P_{3,2}(\tau,\sigma)}{\partial \tau} = \frac{1}{2} - 3\sigma + 3\tau + 3\sigma^2 - 3\tau^2 - 6\sigma^2\tau + 6\sigma\tau^2$$

into (3.14) that

$$H_2[\mathbf{u}^{n+1}] - H_2[\mathbf{u}^n] = -\Delta t\Big\langle \int_0^1 g(\mathbf{U}_\tau^n)\mathrm{d}\tau, \mathbf{v}^n \Big\rangle - \frac{\Delta t^2}{2}\Big\langle \int_0^1 g(\mathbf{U}_\tau^n)\mathrm{d}\tau, \int_0^1 g(\mathbf{U}_\sigma^n)\mathrm{d}\sigma \Big\rangle. \tag{3.15}$$

Combining the results of (3.12), (3.13), and (3.15), we have the desired result. □

Remark 3.2. *Similar as the proof process of Theorem 2.2, it can be verified that the continuous stage RKN Fourier pseudo-spectral scheme* (3.10) *is time reversible. Moreover, we have noticed that the authors in [40] considered the integrating factor technique and the 4th-order (2-stage) Gauss-Legendre Runge-Kutta scheme to propose a symplectic time integration method for three-dimensional nonlinear water waves. This method can sufficiently use the oscillation generated by the spatial discretisation. Moreover, we have observed that the authors in [40] employed the integrating factor technique and the fourth-order (two-stage) Gauss-Legendre Runge-Kutta scheme to develop a symplectic time integration method for three-dimensional nonlinear water waves. This approach efficiently utilizes the oscillations resulting from spatial discretization, and typically yields accurate results at a reasonable computational cost. Perhaps, the combination of our proposed energy-preserving time integrator with the integrating factor technique could lead to a more efficient energy-preserving scheme. This will be considered in our future research.*

Remark 3.3. *In practice, the integrals in the fully discrete scheme usually cannot be easily calculated. Therefore, the s-point Gauss-Legendre formula* $(b_i, c_i)_{i=1}^s$ *will be used to evaluate the integrals*

$$\begin{cases} \mathbf{U}_{c_i}^n = \mathbf{u}^n + c_i\Delta t\mathbf{v}^n + \Delta t^2 \sum\limits_{j=1}^{s} b_j P_{3,2}(c_i, c_j) g(\mathbf{U}_{c_j}^n), \quad i = 1, 2, \ldots, s, \\ \mathbf{u}^{n+1} = \mathbf{u}^n + \Delta t\mathbf{v}^n + \Delta t^2 \sum\limits_{i=1}^{s} b_i(1 - c_i) g(\mathbf{U}_{c_i}^n), \\ \mathbf{v}^{n+1} = \mathbf{v}^n + \Delta t \sum\limits_{i=1}^{s} b_i g(\mathbf{U}_{c_i}^n). \end{cases} \tag{3.16}$$

Since the s-point GL quadrature formula is symmetric, the formula (3.16) *is also symmetric.*

To date, we have developed an energy-preserving fully discrete scheme for solving the two-dimensional nonlinear wave Eqs (1.1) and (1.2). This was achieved by initially semidiscretizing the temporal derivatives using a continuous-stage RKN method, followed by applying the Fourier spectral differential matrix A to approximate the spatial differential operator $\mathcal{A}$. It has been observed that the Fourier pseudo-spectral method for approximating spatial derivatives can achieve spectral precision of order $O(M^{-r})$ provided that the spatial regularity conditions are adequately satisfied.

Assume that $u(t)$ and $v(t)$ represent the exact solution and its derivative of the abstract ODE's system (2.1), while $\mathbf{u}(t)$ and $\mathbf{v}(t)$ denote the exact solution and its derivative of the semi-discrete system (3.7). Additionally, $\mathbf{u}^n$ and $\mathbf{v}^n$ signify the numerical solutions obtained from the continuous

stage RKN Fourier pseudo-spectral scheme (3.10). It follows from inserting the exact solution $\mathbf{u}(t)$ of the semi-discrete system (3.7) into the continuous stage RKN Fourier pseudo-spectral scheme (3.10) that

$$\begin{cases} \mathbf{u}(t_n+\tau\Delta t)=\mathbf{u}(t_n)+\tau\Delta t\mathbf{v}(t_n)+\Delta t^2\int_0^1 P_{3,2}(\tau,\sigma)g(\mathbf{u}(t_n+\sigma\Delta t))\mathrm{d}\sigma+\mathbf{R}^n(\tau),\\ \mathbf{u}(t_{n+1})=\mathbf{u}(t_n)+\Delta t\mathbf{v}(t_n)+\Delta t^2\int_0^1(1-\tau)g(\mathbf{u}(t_n+\tau\Delta t))\mathrm{d}\tau,\\ \mathbf{v}(t_{n+1})=\mathbf{v}(t_n)+\Delta t\int_0^1 g(\mathbf{u}(t_n+\tau\Delta t))\mathrm{d}\tau, \end{cases} \tag{3.17}$$

where $\mathbf{R}^n(\tau)\in\mathcal{V}_M$ is the temporal local truncation error. Similar to the analysis of Theorem 2.3, we obtain the estimation for the residual $\mathbf{R}^n(\tau)$ in the following theorem.

Theorem 3.3. *Suppose that the semi-discrete system* (3.7) *is well-posed and satisfies* $\mathbf{u}(t)\in C^2([t_0,T])$ *and the nonlinear function* $f'\in L^\infty([t_0,T])$. *Then, the local truncation error* $\mathbf{R}^n(\tau)$ *could be estimated as*

$$\|\mathbf{R}^n(\tau)\|\le\tilde{C}\Delta t^4,\qquad 0\le\tau\le 1, \tag{3.18}$$

where $\tilde{C}$ *is a constant and independent of* Δt.

Proof. The details of the proof are similar to the process of Theorem 2.3, so we omit the details. □

Letting

$$e^n=u(t_n)-\mathbf{u}^n,\quad \eta^n=v(t_n)-\mathbf{v}^n,\quad \mathbf{e}^n=\mathbf{u}(t_n)-\mathbf{u}^n,\quad \boldsymbol{\eta}^n=\mathbf{v}(t_n)-\mathbf{v}^n,\quad \mathbf{E}_\tau^n=\mathbf{u}(t_n+\tau\Delta t)-\mathbf{U}_\tau^n, \tag{3.19}$$

and subtracting (3.10) from (3.17), we obtain

$$\begin{cases} \mathbf{E}_\tau^n=\mathbf{e}^n+\tau\Delta t\boldsymbol{\eta}^n+\Delta t^2\int_0^1 P_{3,2}(\tau,\sigma)\Big(g(\mathbf{u}(t_n+\sigma\Delta t)-g(\mathbf{U}_\sigma^n))\Big)\mathrm{d}\sigma+\mathbf{R}^n(\tau),\\ \mathbf{e}^{n+1}=\mathbf{e}^n+\Delta t\boldsymbol{\eta}^n+\Delta t^2\int_0^1(1-\tau)\Big(g(\mathbf{u}(t_n+\tau\Delta t))-g(\mathbf{U}_\tau^n)\Big)\mathrm{d}\tau,\\ \boldsymbol{\eta}^{n+1}=\boldsymbol{\eta}^n+\Delta t\int_0^1\Big(g(\mathbf{u}(t_n+\tau\Delta t))-g(\mathbf{U}_\tau^n)\Big)\mathrm{d}\tau. \end{cases} \tag{3.20}$$

We suppose the two-dimensional nonlinear wave Eqs (1.1) and (1.2) are well-posed. Subsequently, we present the error estimation for the fully discrete scheme (3.10) as detailed in the following theorem.

Theorem 3.4. *If the exact solution* $u(x,y,t)$ *of the two-dimensional nonlinear wave Eqs* (1.1) *and* (1.2) *satisfies* $u(x,y,t)\in C^2([t_0,T],\mathcal{B})$, *and the nonlinear function* $f(\cdot)$ *satisfies* $f'\in L^\infty([t_0,T],\mathcal{B})$, *then under the limitation of* $0<\Delta t\le h_0$ *with a sufficiently small* h_0 *such that* $h_0\|A\|<1$, *we obtain the error bounds*

$$\|e^n\|+\Delta t\|\eta^n\|\lesssim M^{-r}+\Delta t^4. \tag{3.21}$$

Here, we should point out that $A\lesssim B$ *means there is a constant* C *such that* $A\le CB$, *and* $M=M_1=M_2$ *is the spatial grid scale. Moreover, the constant* C *depends on* T, *but is independent of* $M,\|A\|$, *and* Δt.

Proof. The concept of the temporal-spatial error splitting method suggests that

$$\begin{aligned} \|e^n\| + \Delta t\|\boldsymbol{\eta}^n\| \leq\ & \|u(t_n) - \mathbf{u}(t_n)\| + \Delta t\|v(t_n) - \mathbf{v}(t_n)\| + \|\mathbf{u}(t_n) - \mathbf{u}^n\| + \Delta t\|\mathbf{v}(t_n) - \mathbf{v}^n\| \\ \leq\ & O(M^{-r}) + \|\mathbf{e}^n\| + \Delta t\|\boldsymbol{\eta}^n\|. \end{aligned} \tag{3.22}$$

Therefore, to obtain the accuracy of the fully discrete scheme, it is essential to concentrate on the analysis of temporal accuracy. Taking norms on both sides of (3.20) leads to

$$\begin{cases} \|\mathbf{E}_\tau^n\| \lesssim \|\mathbf{e}^n\| + \tau\Delta t\|\boldsymbol{\eta}^n\| + \Delta t^2\|A\| \displaystyle\int_0^1 \|\mathbf{E}_\sigma^n\|\mathrm{d}\sigma + O(\Delta t^4), \\ \|\mathbf{e}^{n+1}\| \lesssim \|\mathbf{e}^n\| + \Delta t\|\boldsymbol{\eta}^n\| + \Delta t^2\|A\| \displaystyle\int_0^1 (1-\tau)\|\mathbf{E}_\tau^n\|\mathrm{d}\tau, \\ \|\boldsymbol{\eta}^{n+1}\| \lesssim \|\boldsymbol{\eta}^n\| + \Delta t\|A\| \displaystyle\int_0^1 \|\mathbf{E}_\tau^n\|\mathrm{d}\tau. \end{cases} \tag{3.23}$$

Then, under the restriction of the time step size $\Delta t \leq h_0$ with sufficiently small h_0 satisfying $h_0\|A\| < 1$, the first inequality of (3.23) results in

$$\int_0^1 \|\mathbf{E}_\tau^n\|\mathrm{d}\tau \lesssim \|\mathbf{e}^n\| + \Delta t\|\boldsymbol{\eta}^n\| + O(\Delta t^4). \tag{3.24}$$

Summing up the last two inequalities of (3.23), we have

$$\|\mathbf{e}^{n+1}\| + \Delta t\|\boldsymbol{\eta}^{n+1}\| \lesssim\ \|\mathbf{e}^n\| + 2\Delta t\|\boldsymbol{\eta}^n\| + \Delta t^2\|A\| \int_0^1 \|\mathbf{E}_\tau^n\|\mathrm{d}\tau. \tag{3.25}$$

Moreover, the third inequality of (3.23) results in

$$\|\boldsymbol{\eta}^n\| \lesssim\ \Delta t\|A\| \sum_{k=0}^{n-1} \int_0^1 \|\mathbf{E}_\tau^k\|\mathrm{d}\tau. \tag{3.26}$$

Combining (3.25) and (3.26), we obtain

$$\|\mathbf{e}^{n+1}\| + \Delta t\|\boldsymbol{\eta}^{n+1}\| \lesssim\ \|\mathbf{e}^n\| + \Delta t\|\boldsymbol{\eta}^n\| + \Delta t^2\|A\| \sum_{k=0}^{n} \int_0^1 \|\mathbf{E}_\tau^k\|\mathrm{d}\tau. \tag{3.27}$$

The mathematical induction will be an efficient approach to prove the result of the theorem.
Step I. Letting $n = 0$ in (3.24) and noticing $\mathbf{e}^0 = 0, \boldsymbol{\eta}^0 = 0$, we have

$$\int_0^1 \|\mathbf{E}_\tau^0\|\mathrm{d}\tau = O(\Delta t^4).$$

Furthermore, noticing the limitation of the time step size again, the inequality (3.25) leads to

$$\|\mathbf{e}^1\| + \Delta t\|\boldsymbol{\eta}^1\| \lesssim \Delta t^2\|A\| \int_0^1 \|\mathbf{E}_\tau^0\|\mathrm{d}\tau = O(\Delta t^4).$$

Step II. Now, we assume that the estimation (3.21) is valid for $1 \le n \le m-1$. That is,

$$\|\mathbf{e}^n\| + \Delta t\|\boldsymbol{\eta}^n\| = O(\Delta t^4), \qquad n = 1, 2, \ldots, m-1.$$

Then, by mathematical induction, we only need to verify that the estimation (3.21) is still valid for $n = m$. Setting $n = m-1$ in (3.27) and using the above assumptions leads to

$$\begin{aligned}\|\mathbf{e}^m\| + \Delta t\|\boldsymbol{\eta}^m\| \lesssim\ & \|\mathbf{e}^{m-1}\| + \Delta t\|\boldsymbol{\eta}^{m-1}\| + \Delta t^2\|A\| \sum_{k=0}^{m-1} \int_0^1 \|\mathbf{E}_\tau^k\| \mathrm{d}\tau \\ =\ & O(\Delta t^4) + \Delta t^2\|A\| \sum_{k=0}^{m-1} O(\Delta t^4) \lesssim \Delta t^4.\end{aligned}$$

Therefore, the proof of (3.21) is completed. □

Remark 3.4. *The conclusion of Theorem 3.4 indicates that the continuous-stage RKN Fourier pseudo-spectral scheme has at least fourth-order accuracy in the temporal domain. Owing to the temporal reversibility of the scheme* (3.10)*, the forthcoming numerical experiments demonstrate that the proposed energy-preserving continuous-stage RKN Fourier pseudo-spectral scheme* (3.10) *can achieve sixth-order convergence in time.*

Remark 3.5. *In general, the preservation of energy typically ensures the stability of the fully discrete scheme. The analysis process of Theorem 3.2 demonstrates that the proposed energy-preserving scheme* (3.10) *is unconditionally stable. However, according to the result presented in Theorem 3.4, it can be concluded that the continuous stage RKN Fourier pseudo-spectral scheme* (3.10) *exhibits convergence under the condition* $0 < \Delta t \le h_0$ *with* $h_0\|A\| < 1$*. In fact, the constraint* $h_0\|A\| < 1$ *corresponds to the CFL condition, as the differential matrix is intrinsically linked to the spatial discretization scale.*

4. Numerical experiments

We observe that the weight function $P_{3,2}(\tau, \sigma)$ of the the continuous stage RKN Fourier pseudo-spectral scheme defined in Definition 2.1 is a cubic binary polynomial. Hereafter, the continuous stage RKN Fourier pseudo-spectral scheme will be denoted as **EP3-FP**. In this section, we will calculate the two-dimensional Klein-Gordon equation and the two-dimensional sine-Gordon equation to verify the precision, the efficiency, and the energy preservation of the derived EP3-FP scheme. Additionally, the following energy-preserving time integrators are chosen for comparison:

- *AVF*: the energy-preserving second-order averaged vector field method (see, e.g., [15, 16]);
- *HEP3*: the symmetric sixth-order energy-preserving integrator constructed by Hairer in [15];
- *SRKN3*: the continuous-stage symplectic RKN method of order six (see, e.g., [34–36]).

The fully discrete scheme is obtained after discretizing the spatial derivatives with the Fourier pseudo-spectral method. We compute the temporal convergence rate by the following formula:

$$\text{Rate} = \log_2 \frac{\text{GE}(h)}{\text{GE}(h/2)} \qquad \text{with} \qquad \text{GE}(h) = \|U(T; h) - u(T; h)\|, \tag{4.1}$$

where the global error GE(h) is the difference of the exact solution $U(T;h)$ with the numerical solution $u(T;h)$ at time T with step h. Moreover, it is known that the exact solution of the two-dimensional sine-Gordon equation could not be explicitly represented. Therefore, we will use the posterior error (see, e.g., [9, 20]) to calculate the convergence rate, i.e.,

$$\text{Rate} = \log_2 \frac{\text{PE}(h)}{\text{PE}(h/2)} \qquad \text{with} \qquad \text{PE}(h) = \|u(T;h) - u(T;h/2)\|. \tag{4.2}$$

Furthermore, it is important to emphasize that the energy-preserving continuous-stage RKN time-stepping method introduced in this work, as well as the numerical methods selected for comparison, are closely associated with nonlinear integrals. To approximate these nonlinear integrals, the four-point Gauss-Legendre quadrature formula will be employed in numerical simulation.

Problem 1. Consider the two-dimensional nonlinear periodic Klein-Gordon equation (see, e.g., [18])

$$\begin{cases} \dfrac{\partial^2 u}{\partial t^2} - c^2\left(\dfrac{\partial^2 u}{\partial x^2} + \dfrac{\partial^2 u}{\partial y^2}\right) + au + bu^3 = f(x,y,t), \quad (x,y) \in (-2,2)\times(-2,2), \quad t \in (0,100], \\ u(x,y,0) = \cos\left(\pi(x+y)\right), \quad \dfrac{\partial u(x,y,0)}{\partial t} = \pi \sin\left(\pi(x+y)\right), \quad (x,y) \in [-2,2]\times[-2,2], \end{cases} \tag{4.3}$$

with the right-hand function $f(x,y,t) = \cos\left(\pi(x+y-t)\right) + \cos^3\left(\pi(x+y-t)\right)$. The exact solution is given by

$$u(x,y,t) = \cos\left(\pi(x+y-t)\right).$$

We choose the parameters as $a = 1, b = 1$, and $c^2 = \frac{1}{2}$. In Table 1, we list the errors and the corresponding convergence rates of the proposed EP3-FP scheme by varying the spatial and temporal step sizes. In Figure 1, we set the spatial grid scales as $M = M_x = M_y = 64$, and the logarithms of the global errors $\log_{10}(GE)$ against different time steps and the CPU times are plotted in Figure 1(a) and Figure 1(b), respectively. The logarithms of the energy errors of the EP3-FP scheme are plotted in Figure 1(b), which show that the proposed scheme is energy-preserving. The numerical results in Table 1 and Figure 1(a) illustrate that the proposed EP3-FP scheme achieves sixth-order temporal accuracy. Figure 1(c) shows that the EP3 time-stepping scheme has better computational efficiency than the chosen numerical methods.

Table 1. The global errors and temporal convergence rates of the "**EP3-FP**" scheme for solving Problem 1.

Error	$\Delta t = 0.08$	$\Delta t = 0.04$	$\Delta t = 0.02$	$\Delta t = 0.01$
$M = 8$	4.7423E − 08	7.4247E − 10	1.1636E − 11	2.0639E − 13
Rate	–	**5.9971**	**5.9957**	**5.8170**
$M = 16$	5.5603E − 08	8.7012E − 10	1.3624E − 11	2.4547E − 13
Rate	–	**5.9978**	**5.9970**	**5.7944**
$M = 32$	5.9563E − 08	9.3049E − 10	1.4581E − 11	2.4236E − 13
Rate	–	**6.0003**	**5.9958**	**5.9108**
$M = 64$	5.9670E − 08	9.3484E − 10	1.4611E − 11	2.4836E − 13
Rate	–	**5.9962**	**5.9996**	**5.8785**

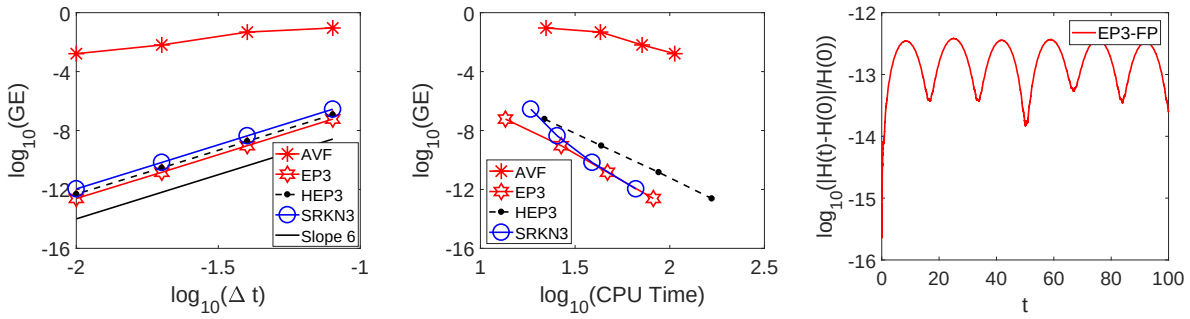

(a) (b) (c)

Figure 1. Results for Problem 1 with $M_x = M_y = 64$. (**a**) the log-log plot of the global error against different steps h. (**b**) the log-log plot of the global error against CPU time. (**c**) the log plot of the relative energy error against integrate time with $H(0) = 123.9352528130722$.

Problem 2. Consider the two-dimensional sine-Gordon equations (see, e.g., [23, 26, 27])

$$\frac{\partial^2 u}{\partial t^2} - \kappa^2 \left(\frac{\partial^2 u}{\partial x^2} + \frac{\partial^2 u}{\partial y^2} \right) + \sin\left(u(x, y, t)\right) = 0, \quad (x, y) \in [-1, 1] \times [-1, 1], \quad t \in (0, 100], \tag{4.4}$$

with the dimensionless parameter $\kappa = 1/20$, and the initial conditions

$$u(x, y, 0) = 4 \arctan\Big(\exp\left(3 - \sqrt{x^2 + y^2}/\kappa^2\right)\Big), \qquad \frac{\partial u(x, y, 0)}{\partial t} = 0.$$

Suppose that the two-dimensional sine-Gordon Eq (4.4) is equipped with periodic boundary conditions. Some snapshots of the numerical solution by the EP3-FP scheme are shown in Figure 2. These results demonstrate that the proposed EP3-EP scheme can efficiently simulate the two-dimensional sine-Gordon Eq (4.4) in a relatively long time domain. Moreover, it can be clearly observed from Figure 2 that the ring soliton shrinks during the initial stage, and oscillations and radiations have emerged by $t = 34.2$. Furthermore, the graphs also illustrate that the pulse simulated by the 2D sine-Gordon equation exhibits periodic oscillation. These phenomena are indeed valid, as other numerical methods have been employed to simulate this problem and exhibit similar phenomena. Here, we do not display the graphs obtained by other numerical methods. The numerical data listed in Table 2 demonstrates the convergence rate of the proposed EP3-FP scheme by varying the spatial and temporal step sizes. In Figure 3, after discretizing the spatial derivatives by the Fourier pseudo-spectral method with the fixed spatial mesh grid scales $M = M_x = M_y = 64$, the problem is calculated by a different time-stepping scheme. These phenomena further validate the accuracy, efficiency, and long-term energy conservation of the EP3-FP scheme.

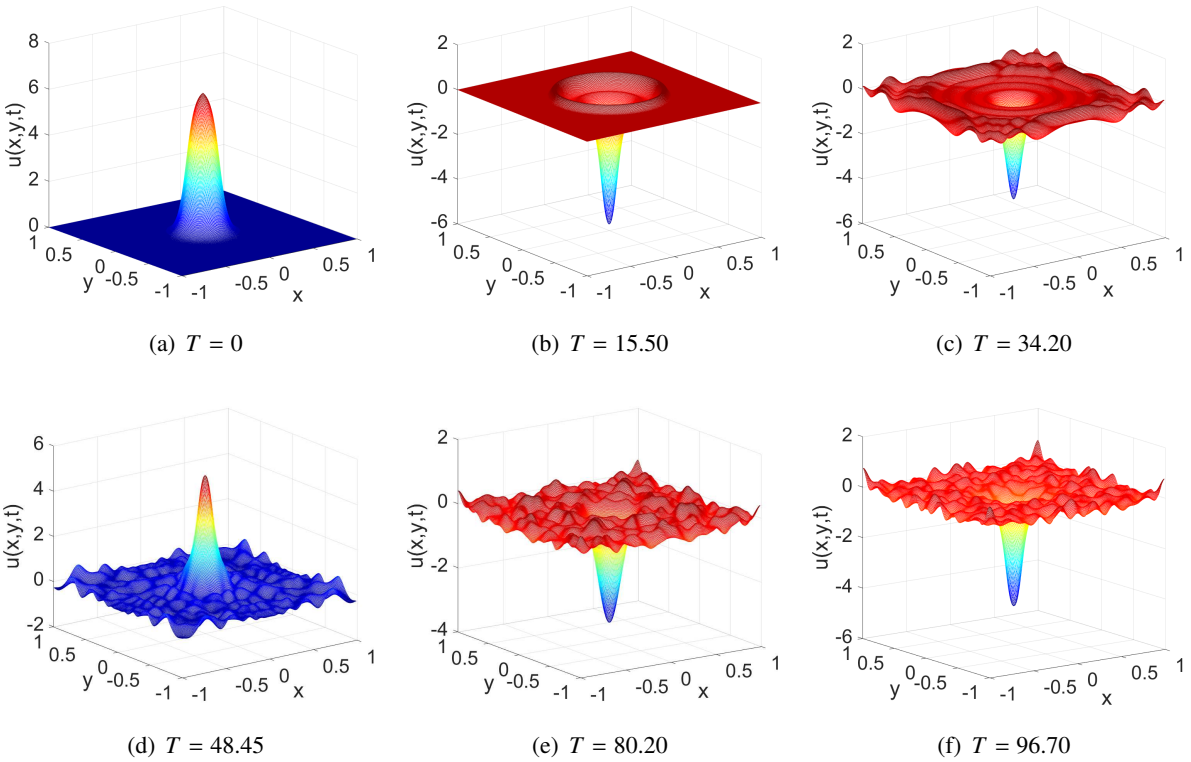

(a) $T = 0$ (b) $T = 15.50$ (c) $T = 34.20$

(d) $T = 48.45$ (e) $T = 80.20$ (f) $T = 96.70$

Figure 2. Snapshots of the numerical solution of the proposed EP3-FP scheme for solving Problem 2 at different times with the spatial mesh grid scales $M = M_x = M_y = 256$ and time step size $\Delta t = 0.01$.

Table 2. The posterior errors and temporal convergence rates of the "**EP3-FP**" scheme for solving Problem 2.

Error	$\Delta t = 0.4$	$\Delta t = 0.2$	$\Delta t = 0.1$	$\Delta t = 0.05$
$M = 8$	5.0772E − 06	8.1347E − 08	1.2794E − 09	1.9459E − 11
Rate	–	**5.9638**	**5.9906**	**6.0388**
$M = 16$	3.4833E − 05	5.6543E − 07	8.9029E − 09	1.4501E − 10
Rate	–	**5.9449**	**5.9889**	**5.9401**
$M = 32$	3.0811E − 04	5.3090E − 06	8.5278E − 08	1.3415E − 09
Rate	–	**5.8588**	**5.9601**	**5.9902**
$M = 64$	1.8629E − 03	2.9562E − 05	4.7003E − 07	7.3794E − 09
Rate	–	**5.9777**	**5.9748**	**5.9931**

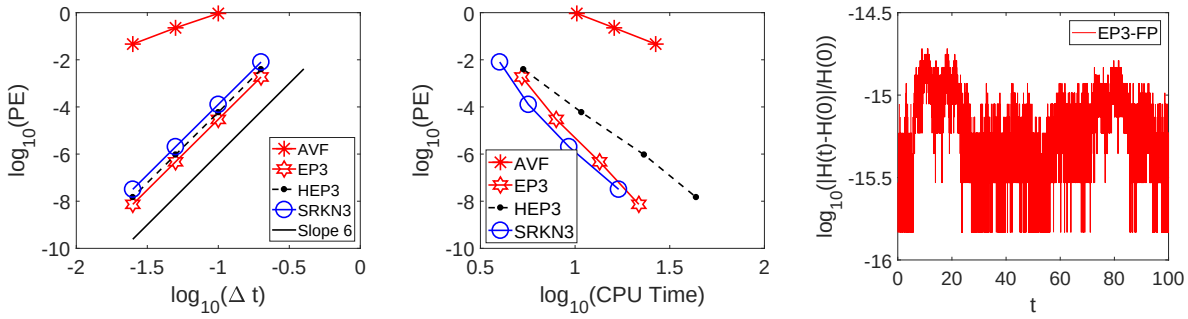

(a) (b) (c)

Figure 3. Results for Problem 2 with $M_x = M_y = 64$. (**a**) the log-log plot of the posterior error against different steps h. (**b**) the log-log plot of the posterior error against CPU time. (**c**) the log plot of the relative energy error against integrate time with $H(0)$=0.377193865036316.

5. Conclusions

In this paper, based on the blend of the energy-preserving continuous-stage RKN time integrator with the Fourier pseudo-spectral spatial discretization, we presented a novel energy-preserving and symmetric fully discrete scheme for solving the two-dimensional nonlinear wave equations. The discrete energy of the two-dimensional nonlinear wave Eqs (1.1) and (1.2) is well conserved by the proposed scheme. Meanwhile, another significant discovery is that the derived EP3-FP scheme can achieve sixth-order temporal accuracy under the low regularity assumption $u \in C^2([t_0, T], \mathcal{B})$. Numerical experiments are presented to illustrate the accuracy, efficiency, and long-term energy conservation of the derived EP3-FP scheme.

In light of a similar process, the derived EP3-FP scheme could be generalized to investigate other Hamiltonian PDEs, including the fractional nonlinear Hamiltonian wave equation, the Klein-Gordon equation with weak nonlinearity, the Klein-Gordon equation in the nonrelativistic limit regime, and the Klein-Gordon-Zakharov system.

Author contributions

Dongjie Gao wrote the main manuscript. Peiguo Zhang prepared numerical experiments. Longqin Wang, Zhenlong Dai and Yonglei Fang made the corrections. All the authors have agreed and given their consent for the publication of this research paper.

Use of Generative-AI tools declaration

The authors declare they have not used Artificial Intelligence (AI) tools in the creation of this article.

Acknowledgments

The work is supported by the Natural Science Foundation of China under Grant 11801280 and 12071419, the Natural Science Foundation of the Jiangsu Higher Education Institutions under Grant 21KJD110002, the Natural Science Foundation of Shandong Province under Grant ZR2024MA056, the foundation of innovative science and technology for youth in universities of Shandong Province under Grant 2023KJ278.

Conflict of interest

The authors declare no conflict of interest.

References

1. T. Aktosun, F. Demontis, C. Der Mee, Exact solutions to the sine-Gordon equation, *J. Math. Phys.*, **51** (2010), 123521. https://doi.org/10.1063/1.3520596
2. J. Argyris, M. Haase, J. Heinrich, Finite element approximation to two-dimensional sine-Gordon solitons, *Comput. Method. Appl. M.*, **86** (1991), 1–26. https://doi.org/10.1016/0045-7825(91)90136-T
3. Z. Asgari, S. M. Hosseini, Numerical solution of two-dimensional sine-Gordon and MBE models using Fourier spectral and high order explicit time stepping methods, *Comput. Phys. Commun.*, **184** (2013), 565–572. https://doi.org/10.1016/j.cpc.2012.10.009
4. R. Sassaman, A. Biswas, Soliton perturbation theory for phi-four model and nonlinear Klein-Gordon equations, *Commun. Nonlinear Sci.*, **14** (2009), 3239–3249. https://doi.org/10.1016/j.cnsns.2008.12.020
5. L. Brugnano, F. Iavernaro, *Line integral methods for conservative problems*, 1 Ed., New York: Chapman and Hall/CRC, 2016. https://doi.org/10.1201/b19319
6. L. Brugnano, F. Iavernaro, D. Trigiante, Hamiltonian boundary value methods (energy preserving discrete line integral methods), *JNAIAM*, **5** (2010), 17–37.
7. L. Brugnano, G. Caccia, F. Iavernaro, Energy conservation issues in the numerical solution of the semilinear wave equation, *Appl. Math. Comput.*, **270** (2015), 842–870. https://doi.org/10.1016/j.amc.2015.08.078
8. L. Brugnano, F. Iavernaro, D. Trigiante, Energy and quadratic invariants preserving integrators based upon gauss collocation formulae, *SIAM J. Numer. Anal.*, **50** (2012), 2897–2916. https://doi.org/10.1137/110856617
9. H. Y. Cao, Z. Z. Sun, G. H. Gao, A three-level linearized finite difference scheme for the Camassa-Holm equation, *Numer. Meth. Part. D. E.*, **30** (2014), 451–471. https://doi.org/10.1002/num.21819
10. J. Chabassier, P. Joly, Energy preserving schemes for nonlinear Hamiltonian systems of wave equations: application to the vibrating piano string, *Comput. Method. Appl. M.*, **199** (2010), 2779–2795. https://doi.org/10.1016/j.cma.2010.04.013

11. M. Dehghan, A. Shokri, A numerical method for one-dimensional nonlinear Sine-Gordon equation using collocation and radial basis functions, *Numer. Meth. Part. D. E.*, **24** (2008), 687–698. https://doi.org/10.1002/num.20289

12. D. Duncan, Sympletic finite difference approximations of the nonlinear Klein-Gordon equation, *SIAM J. Numer. Anal.*, **34** (1997), 1742–1760. https://doi.org/10.1137/S0036142993243106

13. Y. Gong, Q. Wang, Y. Wang, J. Cai, A conservative Fourier pseudo-spectral method for the nonlinear Schrödinger equation, *J. Comput. Phys.*, **328** (2017), 354–370. https://doi.org/10.1016/j.jcp.2016.10.022

14. P. Guyenne, A. Kairzhan, C. Sulem, Hamiltonian Dysthe equation for three-dimensional deep-water gravity waves, *Multiscale Model. Sim.*, **20** (2022), 349–378. https://doi.org/10.1137/21m1432788

15. E. Hairer, Energy-preserving variant of collocation methods, *JNAIAM*, **5** (2010), 73–84.

16. E. Hairer, G. Wanner, C. Lubich, *Geometric numerical integration: structure-preserving algorithms for ordinary differential equations*, 2 Eds., Berlin: Springer, 2006. https://doi.org/10.1007/3-540-30666-8

17. B. Hou, D. Liang, Energy-preserving time high-order AVF compact finite difference schemes for nonlinear wave equations with variable coefficients, *J. Comput. Phys.*, **421** (2020), 109738. https://doi.org/10.1016/j.jcp.2020.109738

18. B. Hou, D. Liang, The energy-preserving time high-order AVF compact finite difference scheme for nonlinear wave equations in two dimensions, *Appl. Numer. Math.*, **170** (2021), 298–320. https://doi.org/10.1016/j.apnum.2021.07.026

19. D. Kaya, S. El-Sayed, A numerical solution of the Klein-Gordon equation and convergence of the decomposition method, *Appl. Math. Comput.*, **156** (2004), 341–353. https://doi.org/10.1016/j.amc.2003.07.014

20. J. Li, Z. Sun, X. Zhao, A three level linearized compact difference scheme for the Cahn-Hilliard equation, *Sci. China Math.*, **55** (2012), 805–826. https://doi.org/10.1007/s11425-011-4290-x

21. S. Li, L. Vu-Quoc, Finite difference calculus invariant structure of a class of algorithms for the nonlinear Klein-Gordon equation, *SIAM J. Numer. Anal.*, **32** (1995), 1839–1875. https://doi.org/10.1137/0732083

22. C. Liu, J. Li, Z. Yang, Y. Tang, K. Liu, Two high-order energy-preserving and symmetric Gauss collocation integrators for solving the hyperbolic Hamiltonian systems, *Math. Comput. Sim.*, **205** (2023), 19–32. https://doi.org/10.1016/j.matcom.2022.09.016

23. C. Liu, K. Liu, A fourth-order energy-preserving and symmetric average vector field integrator with low regularity assumption, *J. Comput. Appl. Math.*, **439** (2024), 115605. https://doi.org/10.1016/j.cam.2023.115605

24. C. Liu, A. Iserles, X. Wu, Symmetric and arbitrarily high-order Birkhoff-Hermite time integrators and their long-time behaviour for solving nonlinear Klein-Gordon equations, *J. Comput. Phys.*, **356** (2018), 1–30. https://doi.org/10.1016/j.jcp.2017.10.057

25. W. J. Liu, J. B. Sun, B. Y. Wu, Space-time spectral method for the two-dimensional generalized sine-Gordon equation, *J. Math. Anal. Appl.*, **427** (2015), 787–804. https://doi.org/10.1016/j.jmaa.2015.02.057

26. C. Liu, Y. Tang, J. Yu, Y. Fang, High-order symmetric and energy-preserving collocation integrators for the second-order Hamiltonian system, *J. Math. Chem.*, **62** (2024), 330–355. https://doi.org/10.1007/s10910-023-01536-x

27. C. Y. Liu, X. Y. Wu, Continuous trigonometric collocation polynomial approximations with geometric and superconvergence analysis for efficiently solving semi-linear highly oscillatory hyperbolic systems, *Calcolo*, **58** (2021), 6. https://doi.org/10.1007/s10092-020-00394-2

28. C. Liu, X. Wu, Nonlinear stability and convergence of ERKN integrators for solving nonlinear multi-frequency highly oscillatory second-order ODEs with applications to semi-linear wave equations, *Appl. Numer. Math.*, **153** (2020), 352–380. https://doi.org/10.1016/j.apnum.2020.02.020

29. C. Y. Liu, X. Y. Wu, Arbitrarily high-order time-stepping schemes based on the operator spectrum theory for high-dimensional nonlinear Klein-Gordon equations, *J. Comput. Phys.*, **340** (2017), 243–275. https://doi.org/10.1016/j.jcp.2017.03.038

30. C. Y. Liu, X. Y. Wu, The boundness of the operator-valued functions for multidimensional nonlinear wave equations with applications, *Appl. Math. Lett.*, **74** (2017), 60–67. https://doi.org/10.1016/j.aml.2017.04.026

31. C. Y. Liu, X. Y. Wu, W. Shi, New energy-preserving algorithms for nonlinear Hamiltonian wave equation equipped with Neumann boundary conditions, *Appl. Math. Comput.*, **339** (2018), 588–606. https://doi.org/10.1016/j.amc.2018.07.059

32. C. Liu, W. Shi, X. Wu, Numerical analysis of an energy-conservation scheme for two-dimensional hamiltonian wave equations with Neumann boundary conditions, *Int. J. Numer. Anal. Mod.*, **16** (2019), 319–339. https://doi.org/2019-IJNAM-12806

33. W. Shi, K. Liu, X. Wu, C. Liu, An energy-preserving algorithm for nonlinear Hamiltonian wave equations with Neumann boundary conditions, *Calcolo*, **54** (2017), 1379–1402. https://doi.org/10.1007/s10092-017-0232-5

34. W. Tang, J. Zhang, Symplecticity-preserving continuous-stage Runge-Kutta-Nyström methods, *Appl. Math. Comput.*, **323** (2018), 204–219. https://doi.org/10.1016/j.amc.2017.11.054

35. W. Tang, J. Zhang, Symmetric integrators based on continuous-stage Runge-Kutta-Nyström methods for reversible systems, *Appl. Math. Comput.*, **361** (2019), 1–12. https://doi.org/10.1016/j.amc.2019.05.013

36. W. Tang, Y. Sun, J. Zhang, High order symplectic integrators based on continuous-stage Runge-Kutta-Nyström methods, *Appl. Math. Comput.*, **361** (2019), 670–679. https://doi.org/10.1016/j.amc.2019.06.031

37. R. Teman, *Infinite-dimensional dynamical systems in mechanics and physics*, New York: Springer, 1997. http://doi.org/10.1007/978-1-4684-0313-8

38. B. Wang, X. Y. Wu, The formulation and analysis of energy-preserving schemes for solving high-dimensional nonlinear Klein-Gordon equations, *IMA J. Numer. Anal.*, **39** (2019), 2016–2044. https://doi.org/10.1093/imanum/dry047

39. A. Wazwaz, Exact solutions for the generalized sine-Gordon and the generalized sinh-Gordon equations, *Chaos Soliton. Fract.*, **28** (2006), 127–135. https://doi.org/10.1016/j.chaos.2005.05.017

40. L. Xu, P. Guyenne, Numerical simulation of three-dimensional nonlinear water waves, *J. Comput. Phys.*, **228** (2009), 8446–8466. https://doi.org/10.1016/j.jcp.2009.08.015